EGU 2015 "Voyage through scales"

Scale-invariance of sediment patterns - the fingerprint of fundamental drivers

Wolfgang Schlager

"The scientist knows more and more about less and less until he knows everything about nothing" *M.Gandhi*

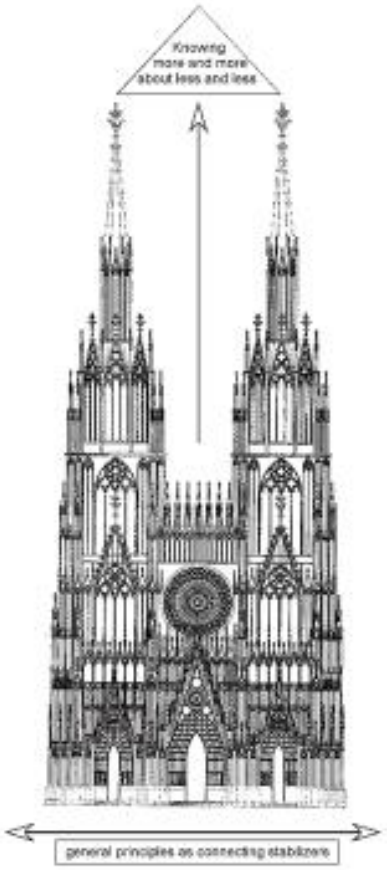

INTRODUCTION Purpose and scope of this lecture were determined by two factors: First, the theme of this convention - "Voyage through scales"; second, Gandhi's warning with respect to the strategy of getting to know more and more by narrowing one's focus. In sedimentary geology, we can find important principles by searching for the opposite of narrow focus: scale-invariant patterns, here illustrated by sediment fans, foresets of non-cohesive sand and rubble, bucket structure of reefs and carbonate platforms and reticulate ecologic patterns including reefs. It must be emphasized though, that in the long run, sedimentary geology progresses best by a blend of both approaches. The gothic cathedral may serve as an illustration of this strategy - building upward by learning more and more about less and less combined with searching for general principles by widening the focus of study. Four examples of scale-invariant sediment patterns and the fundamental drivers behind them are discussed below.

SEDIMENT FANS are well-known example of scale invariance. This summary relies mainly on the excellent study by vanWagoner et al. (2003) and Hoyal et al. (2003). It is important to note that alluvial fans, deltas and turbidite fans exhibit the same overall shape while linear size varies from centimeters to hundreds of kilometers. The invariance with respect to both scale and depositional setting is plausibly explained by the jet model (Allen 1985). The model assumes that the fan deposits develop where a channeled flow is injected into a large body of still water. Dispersion of energy from jets injected in still water occurs by turbulence and lateral expansion of the flow.

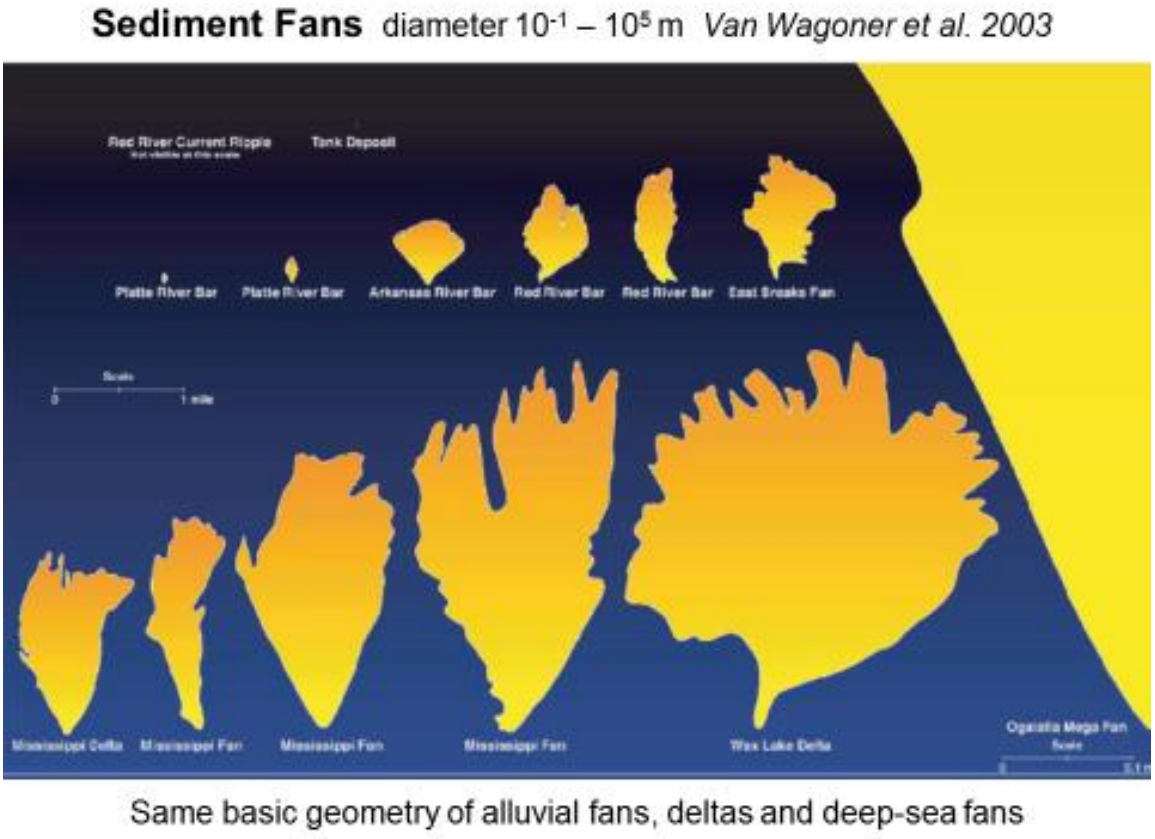

Fig. 1 Outlines of fans ranging in size from centimeters (upper left, below resolution) to fans of >1000 km in diameter (Van Wagoner et al. 2003).

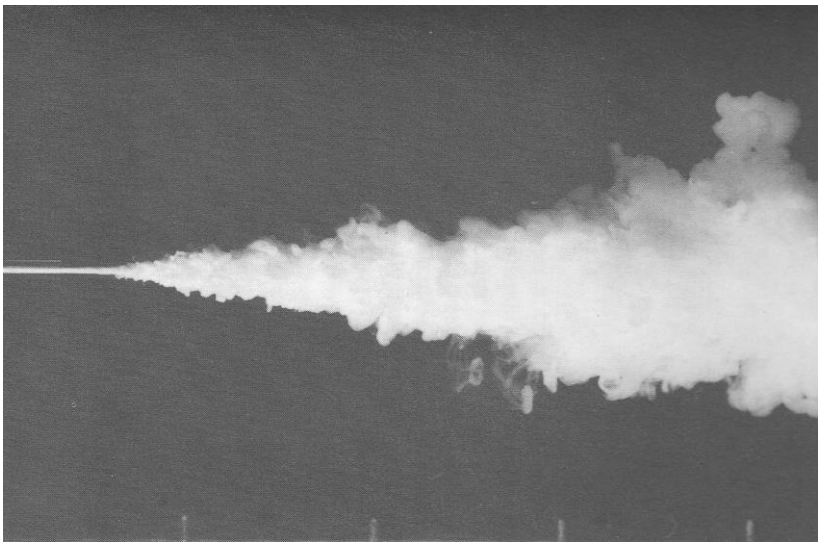

Fig. 2 Dispersion in a jet – the fundamental driver of fan formation. Image shows water with kaolinite (white) being injected into clear quiet water (dark). Widening of diameter and turbulence slows the injected flow and leads to deposition of suspended sediment (Allen 1985).

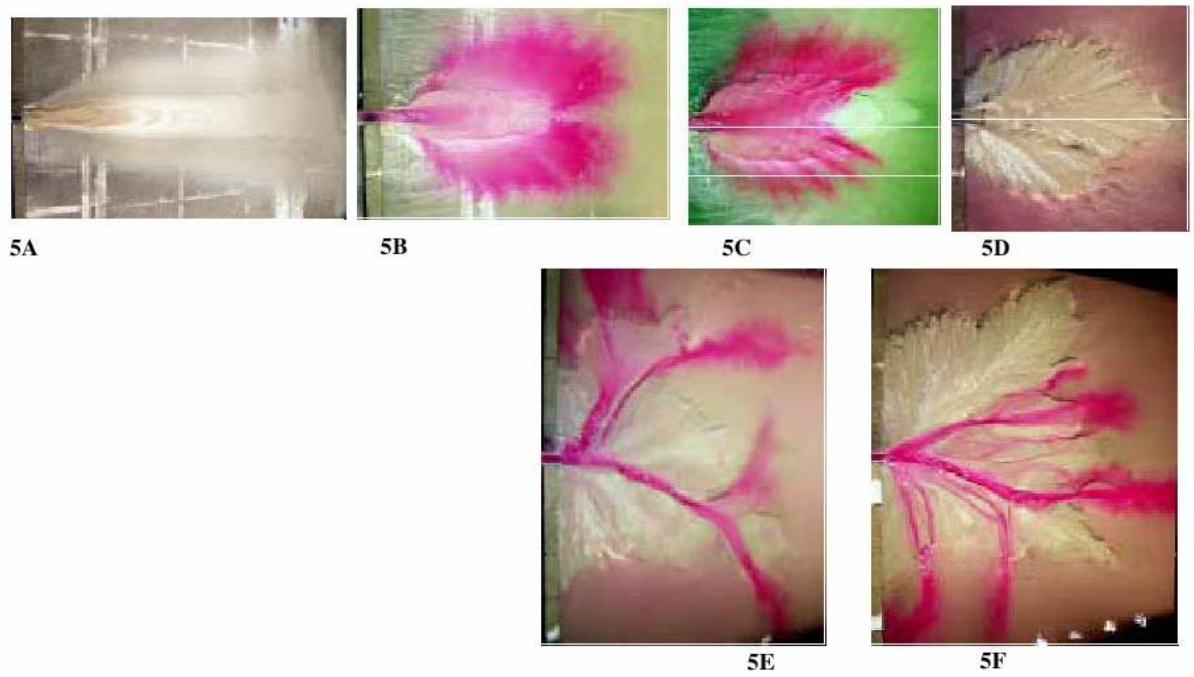

Fig. 3 Flume experiments, partly with colored water, showing the increasing complexity in fan deposits with time and increasing size of the deposit. Basic depositional motif is the elongate white sand lens in 5A. Current-sediment interaction creates flow fingers in 5B. Flow fingers produce mini-lobes of sand arranged in a fan pattern around the original entry point of the jet – "alder leaf fan" in 5D. Finally, avulsions of the main channels in 5E and 5F turn the alder leaf into a maple-leaf fan. (Van Wagoner et al. 2003).

FORESET BEDDING OF NON-COHESIVE SAND AND RUBBLE is another example of scale invariance. The beds are planar and turn flat at the base. This basal curvature frequently has the form of a negative exponential function, probably caused by an exponential decrease of transport capacity or competence when the sediment flows reach the flat basin floor (Adams & Schlager 2000).

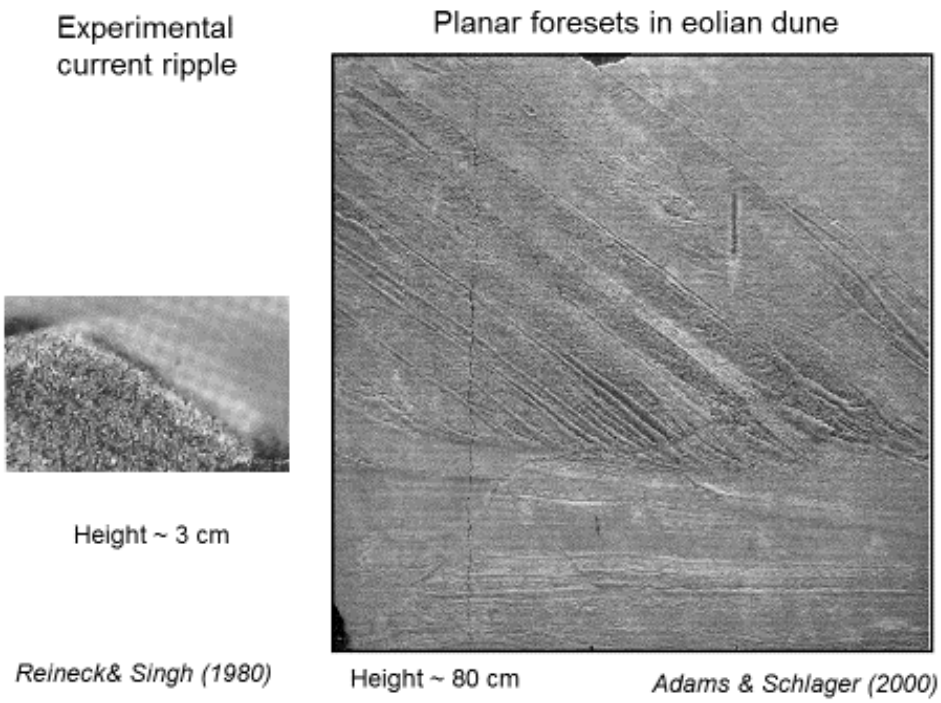

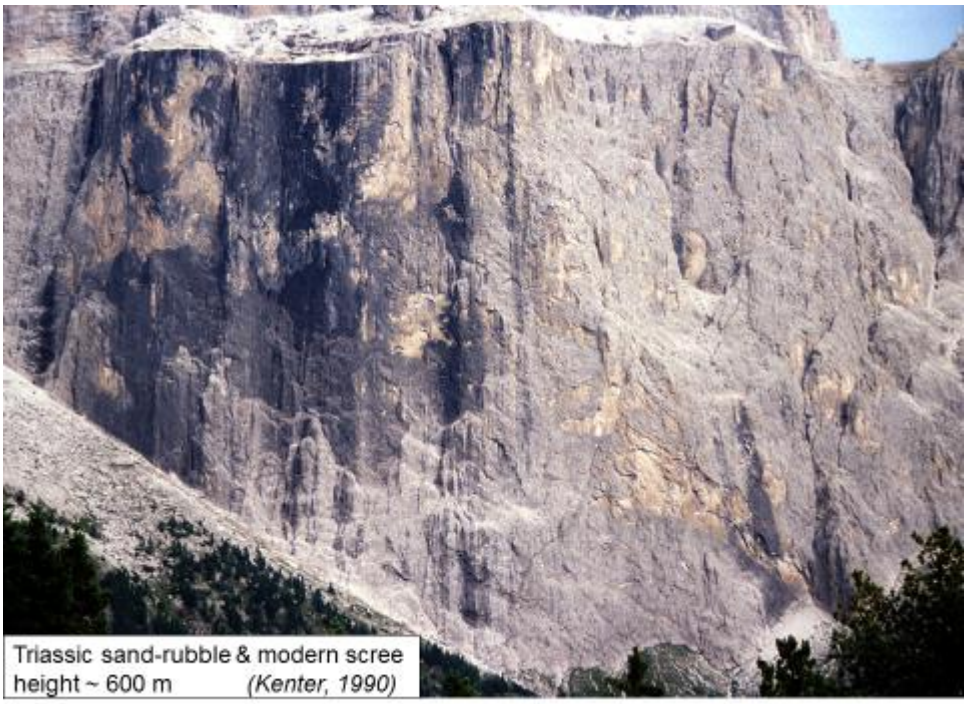

Fig. 4 Planar foresets in size range of 3 cm to 600 m. Upper left: Current ripples in flume experiment (Reineck & Singh, 1980). Upper right: Laquer peel of eolian coastal dune from the Netherlands (Adams & Schlager, 2000). Lower panel: Submarine slope of Triassic carbonate platform in the Dolomites area of the Southern Alps; clinoforms consist of calcareous rubble and sand shed from the platform and microbial crusts produced on the slope (Kenter, 1990; Keim & Schlager, 2001). Microbial structures have only local effect on the slope angle, similar to the minor effect of local vegetation on the morphology of recent scree slopes at the foot of the outcrop (Kenter, 1990).

Sand pile oscillates between
angle of repose & angle of initial yield

Fig. 5 Sand-pile experiments offer an observational basis for the concept of "self-organized criticality" in physics: sand pouring down onto a horizontal surface generates a sand cone. The slope of this cone steepens to the angle of initial yield where numerous small avalanches reduce the slope to stable angle of repose. If supply continues, the system will oscillate by few degrees between angle of initial yield & angle of repose, i.e. in a self-organized critical state (Bak et al. 1988).

BUCKET STRUCTURE OF REEFS AND CARBONATE PLATFORMS The structure of atolls and other tropical carbonate accumulations has been likened to a bucket – a rigid rim of reefs containing a fill of largely unlithified sediment (MacNeil 1954). During the rapid sea-level rise of the last deglaciation, the reef rims frequently kept pace with the rising sea whereas the sedimentation in the lagoons was lagging behind. The resulting "empty buckets" illustrate the crucial role of rim construction in the tropical carbonate factory.

Fig. 6 Bora-Bora Atoll shows typical bucket structure: a deeply eroded volcano as substrate (center), surrounded by shallow-water carbonate deposits consisting of an outer rim of reefs (brownish), an apron of reefs debris and a deep inner lagoon. Darwin already noticed two paradoxes related to atolls: (1) atolls grow best at their outer rims, i.e. at the location of greatest wave force; (2) atolls and most other tropical reefs thrive in low-nutrient water.

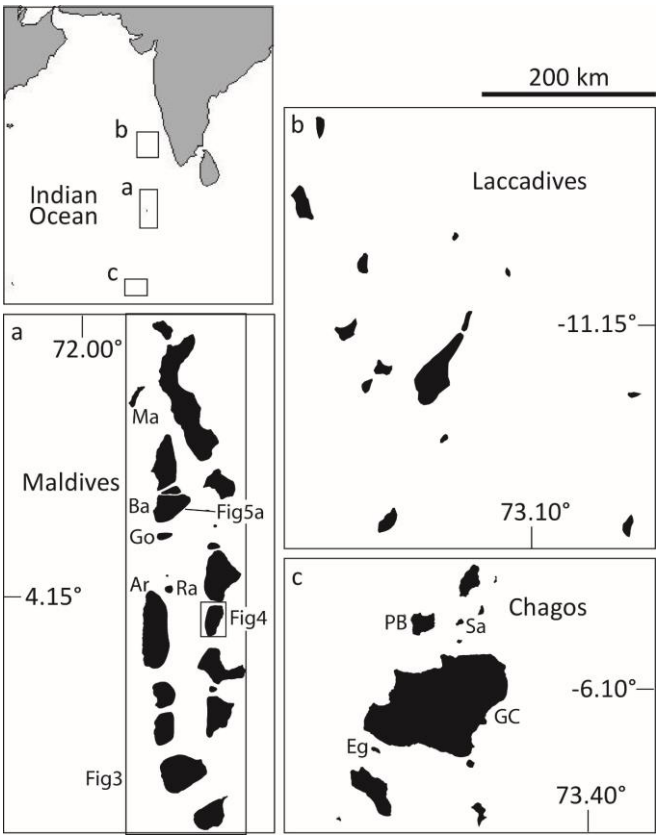

Fig. 7 The Maldive-Chagos-Laccadive archipelagos were chosen by Schlager & Purkis (2013) to assess the size range of buckets and determine their size-frequency characteristics. Choice of this area was governed by the exceptionally well developed patterns of ring reefs, i.e. rings of reefs surrounding deeper lagoons. In addition, self-similarity of ring-reef patterns was common and is reflected in the fact that the Maldivian word "atollon" refers to a large ring-reef consisting of smaller ones (Bates & Jackson 1987,p.43). The largest demonstrable bucket structure of the area is the Maldive archipelago itself, measuring about 60 000 km².

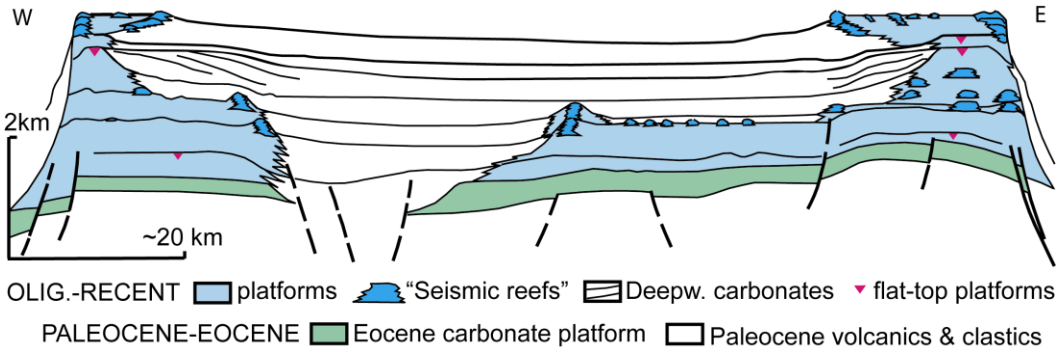

Fig. 8 Bucket structure of the Maldive archipelago as shown by seismics and drilling data (Belopolsky & Droxler, 2013). The structure is ca. 3 km high and 60 000 km² in area. Notice also the bucket structure of the present atolls with mappable reef rims as well as older platforms with mappable reefs rimming the deepwater area of the Inner Sea. The tectonic grabens of the Eocene platform strike oblique to the bucket structure of the archipelago and wedge-out on both ends.

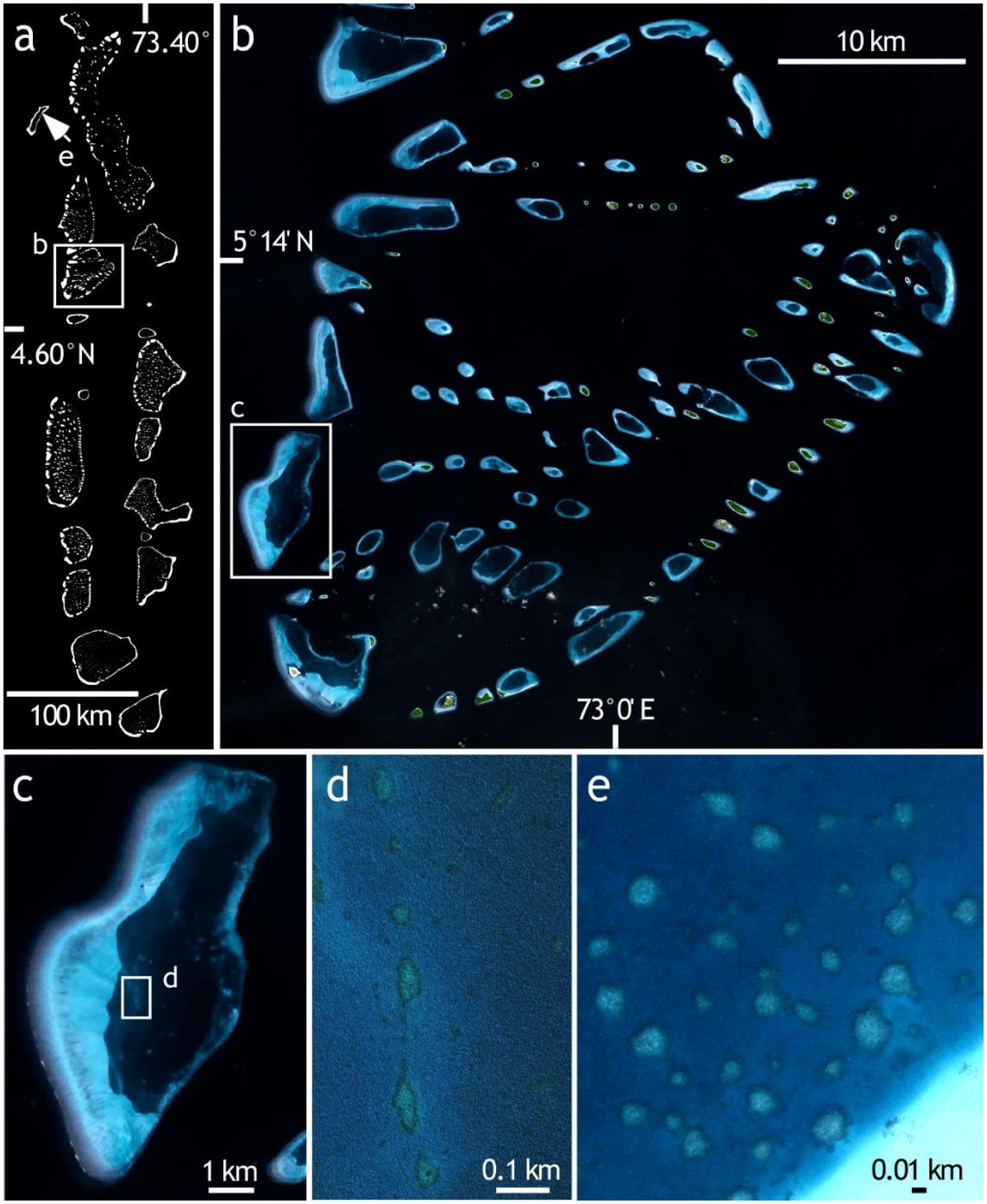

Fig. 9 Remote-sensing data of the seascape of the Maldives clearly illustrate the occurrence of ring reefs with bucket structure in a wide range of scales. The bucket motif ranges from the oval pattern of atolls that constitutes the Maldives (linear size of ???km) down to the ring structure of lagoonal patch reefs of less than 5 m in size. Bucket structures may become strongly asymmetric where strong wave action creates broad debris aprons behind reef rims facing the open ocean, for instance in Figs b & c. (Schlager & Purkis 2013).

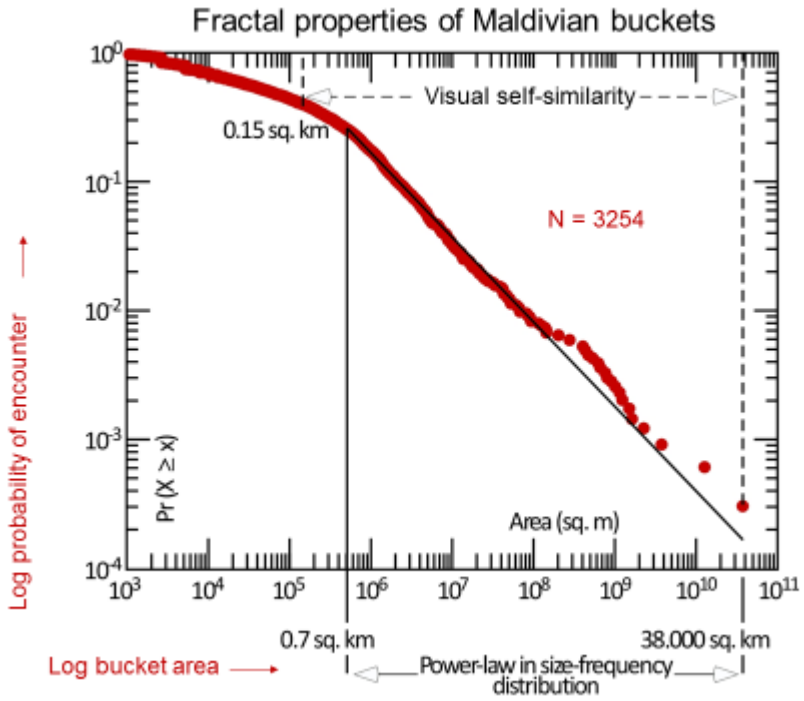

Fig. 10 Self-similarity and fractal appearance of Maldivian ring-reefs is supported by size-frequency analyses. This graph shows log-log plots of all buckets in MCL measured by Schlager & Purkis (2013). The near-linear trend in the range of 0.7-38000 km² indicates an inverse power law linking bucket size to abundance over 2.5 orders of magnitude – in agreement with the interpretation of the ring reefs as statistical fractals. The roll-off on the small end is probably caused by limited resolution of the remote-sensing data.

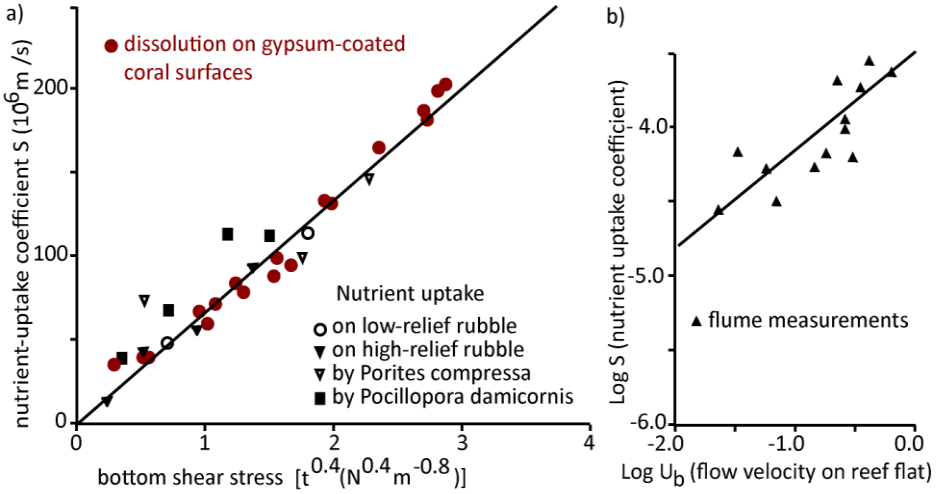

Fig. 11 Biologists and hydrodynamicists produced a very convincing explanation for Darwins paradoxes - the preference of reef communities for low-nutrient waters and for the most turbulent settings within these waters. An early result was that the hydrodynamic roughness of coral surfaces is extremely high and that corals restore this roughness if it is reduced by erosion. An explanation for the high roughness of coral surfaces and for Darwin's paradoxes is offered by the strong positive correlation of bottom shear stress and nutrient by reefs (various experimental data shown above). High bottom shear thins the diffusive boundary layer and thus reduces the biggest obstacle for nutrient uptake by corals. The fact that high shear also increases the rate of dissolution on gypsum-covered corals provides additional support for the diffusive boundary layer as the prime reason for high coral roughness.

RETICULATE REEF-SEDIMENT PATTERNS are related to the bucket structure in the sense that they frequently show the advantage of edge position for reef growth. In addition, they are also influenced by sediment dynamics (Schlager & Purkis, 2014). Traditionally, reticulate reef-sediment patterns in the Holocene have been interpreted as a heritage of antecedent karst formed during lowstands of sea level and there are convincing examples of this link (e.g. Fig.13). However, reticulate reefs on demonstrably flat substrate indicate that there must be other pathways to reticulate patterns.

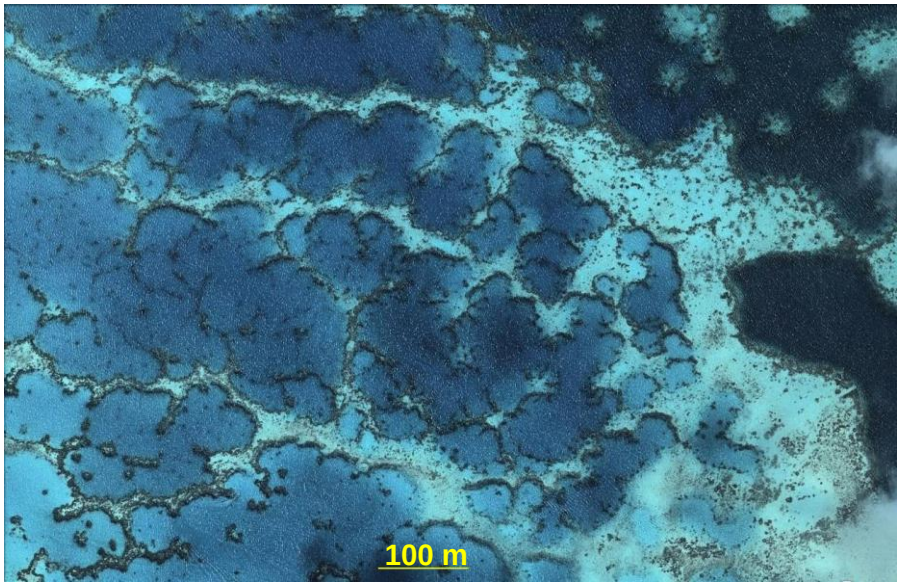

Fig. 12 Reticulate reefs in the lagoon of Maupiti Atoll, South Pacific. Reefs appear as dark ridges, shallow sediment ridges are light blue (facies interpretation after Rankey et al. 2011). Reefs may form reticulate patterns on their own or occupy edge positions of reticulate sediment ridges.

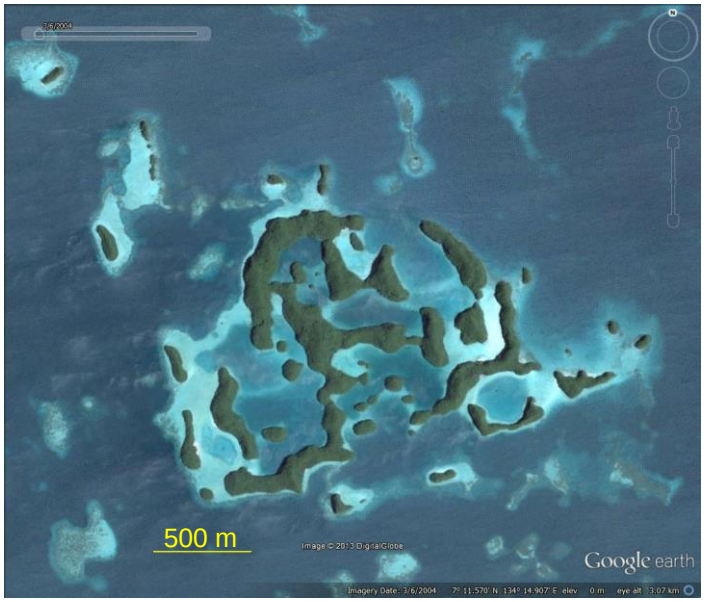

Fig. 13 Palau, W Pacific, tower karst on Tertiary limeststone (forested islands) guides the reticulate pattern of the Quaternary reefs and sediments.

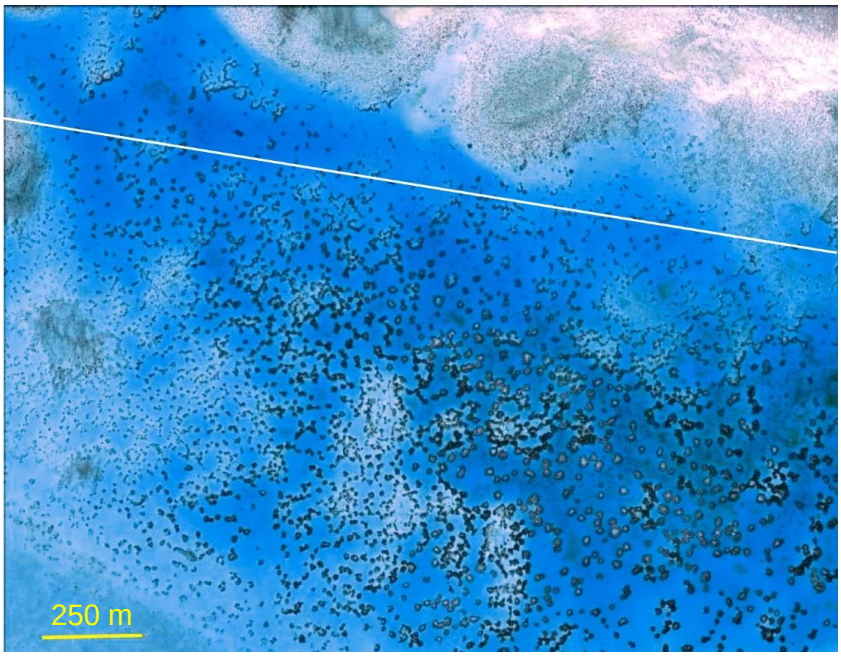

Fig. 14 Scattered buckets beginning to merge to reticulate reefs in the Holocene lagoon of Heron Island, Gt. Barrier Reef. The entire complex is underlain by seismically mapped, flat abrasion surface of early Holocene. Biotic self-organization is a likely cause of the pattern.

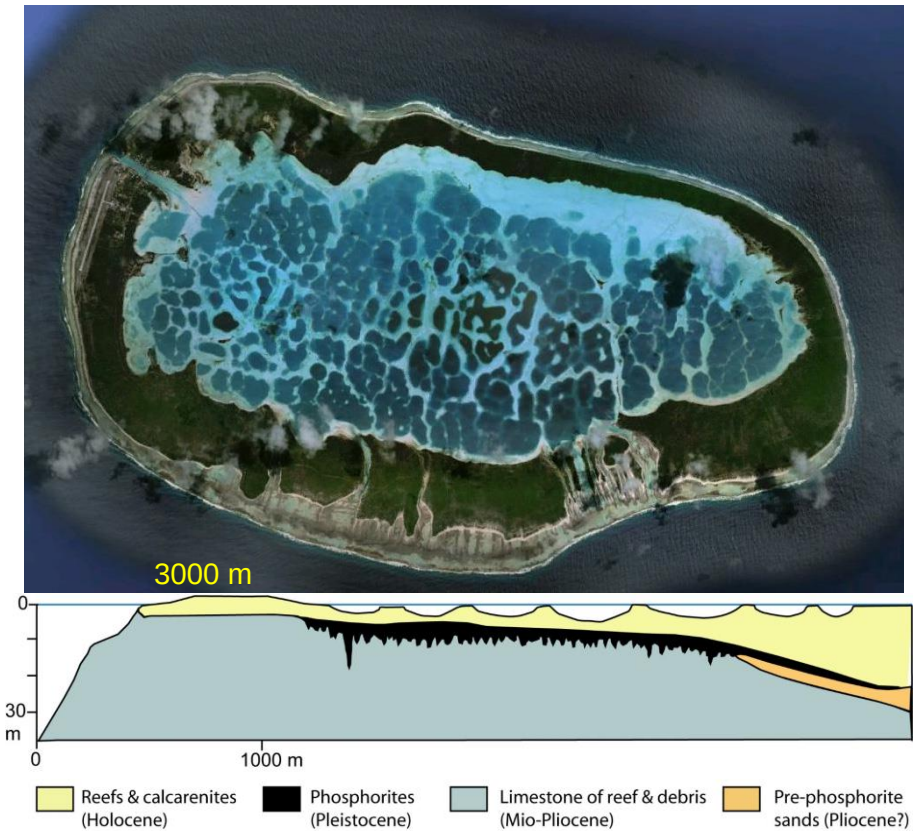

Fig. 15 Matiava Atoll. Above: Reticulate pattern in Holocene lagoon. Below: Cross section of NW part of atoll based on data from phosphate mining. Holocene reticulate pattern rests on smooth surface of Pleistocene phosphate that seals older karst relief. (After Schlager & Purkis 2014).

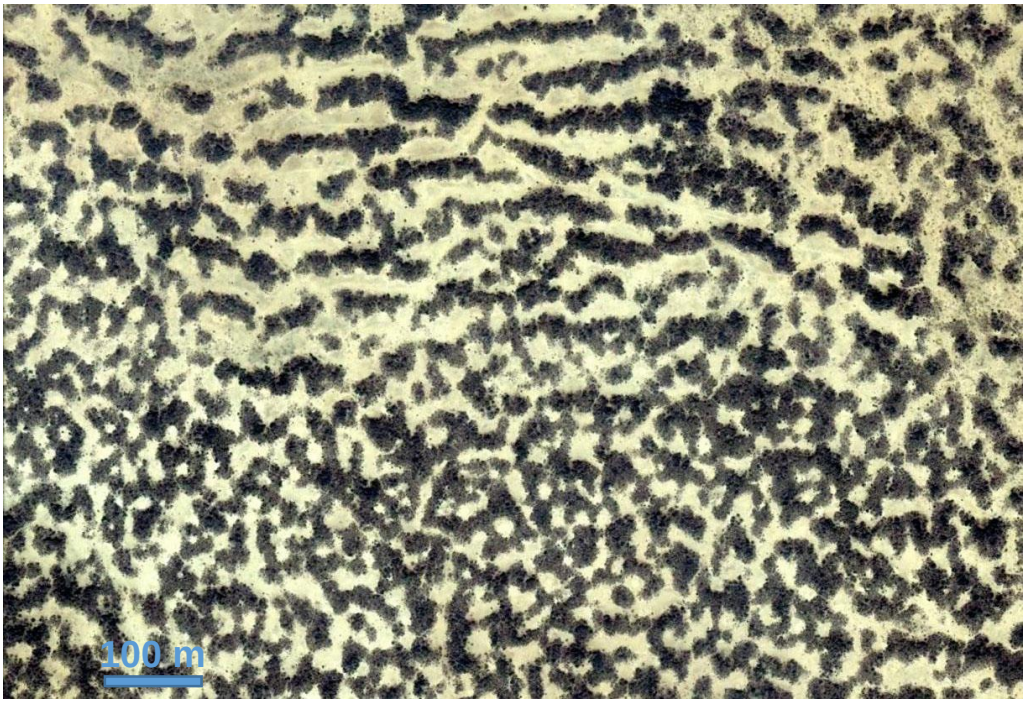

Fig. 16 Biologists report many examples of reticulate vegetation formed by biotic self-organization. This remote-sensing image shows the vegetation of trees and shrubs called "Tigerbush" in Niger. Vegetation organizes itself into reticulate patterns on horizontal surfaces and parallel, horizontal bands on slopes. (After Schlager & Purkis, 2014).

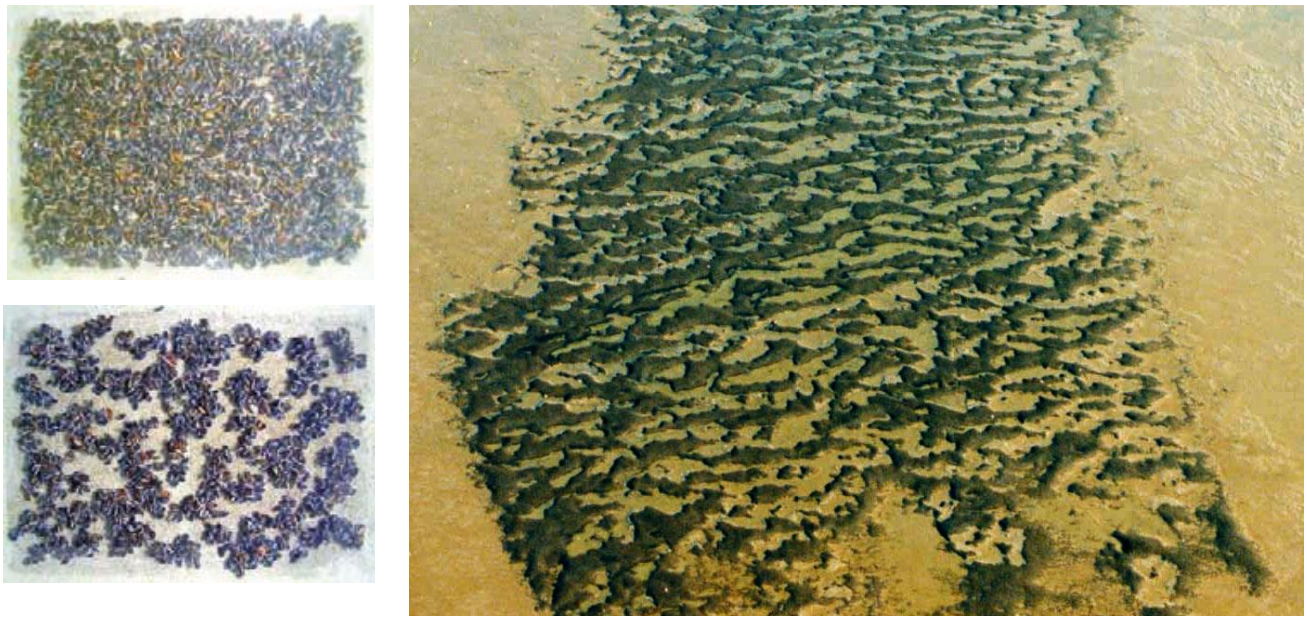

Fig. 17 Reticulate mussel beds (Mytilus edulis). Left: reticulate pattern formed by self-organization of mussels from homogeneous distribution the laboratory. Right: Reticulate patterns of mussel banks on Dutch tidal flats. Width of left panels 80cm, right panel ca. 400 m. (After Van de Koppel et al. 2005, modified).

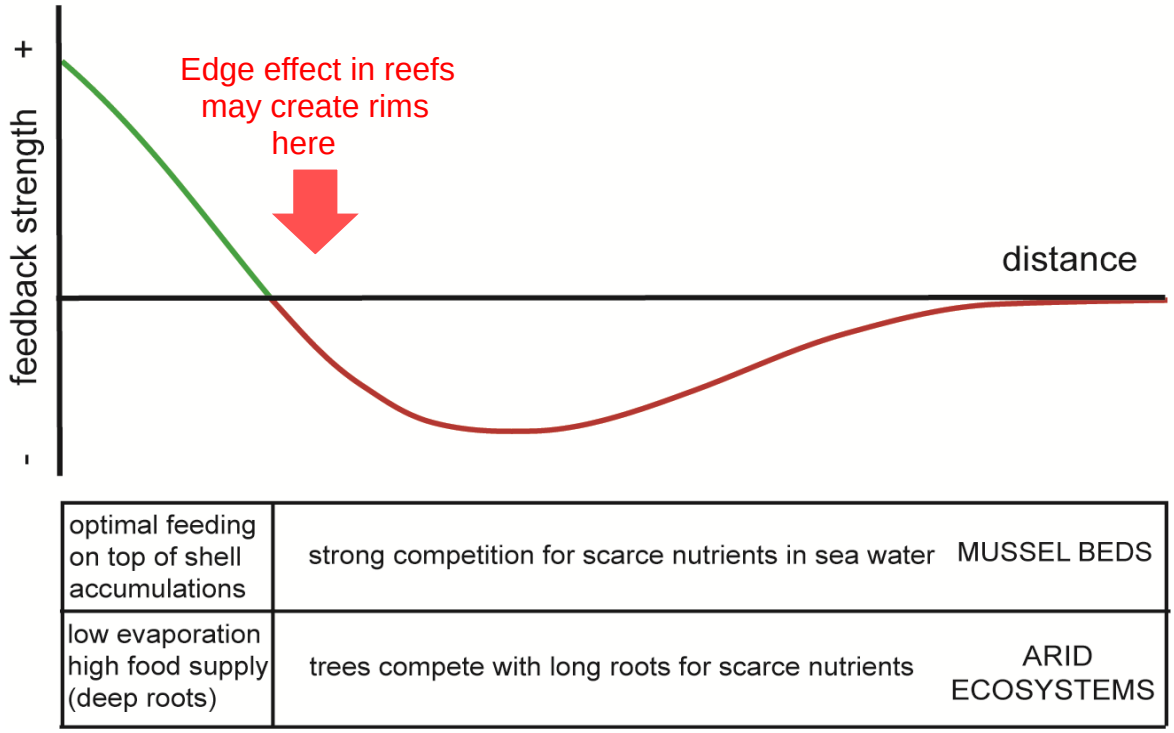

Fig. 18 Reticulate patterns are easily created by models that assume interaction among individuals such that they provide mutual support at short distance and inhibit each other by competing for scarce resources over long distances. This model is analogous to the activator-inhibitor model of Turing for chemical substances. The Turing model creates rather sharp boundaries, such as edges in reef environments. We propose as a working hypothesis that the favored edge position leads to preferred growth of reef-building organisms at the crossover from the domain of mutual support to the domain of mutual inhibition.

SUMMARY. It is instructive to briefly look at the four examples of scale invariance in comparison. Fig. 19 provides some crucial data. Arguably the most important conclusion is that the domain of scale invariance of all examples extends down to the realm of centimeters to meters in linear size, i.e. the realm of laboratory experiments. This result is in line with the conjecture of Paola et al. (2009) that geomorphic experiments are so “unreasonably effective” because the experimental scale is part of the natural size range of the respective phenomena.

EXAMPLE	RANGE INVARIANCE	DRIVER
Fans	10^{-2} - 10^{5} m	energy-dispersion in jet
Foresets	10^{-2} - 10^{3} m	self-organized criticality of debris
Buckets	10^{0} - 10^{5} m	biotic self-org. via favored edge position
Reticulate mussel beds	10^{-1} - 10^{2} m	biotic self-organization via Turing model

Fig. 19 Summary of case studies. Reticulate patterns are only represented by the example of mussel beds because of the directly observable link to biotic self-organization. Reticulate reef-sediment patterns have a wider range of scale-invariance but the driving mechanism is less well constrained. The lower limit of observed scale-invariance of all examples lies in the domain of laboratory experiments.

REFERENCES

Adams EW & Schlager W 2000 J Sed Res v70, 814-828

Allen JRL 1985 Principles of Physical Sedimentology (Allen & Unwin) London

Bak P, Tang C & Wiesenfeld K 1988 Physical Review A v38, 364-374

Bates AL & Jackson JA 1987 Glossary of Geology (3rd ed) Amer. Geol. Inst.

Belopolsky AV & Droxler AW 2004 AAPG Studies in Geology v49, 1-46

Hearn CJ, Atkinson MJ & Falter JL 2001 Coral Reefs v20, 347-356

Hoyal DCJD et al. 2003 AAPG Search & Discovery # 90013

Keim L & Schlager W 2001 Sed Geol v139, 261-283

Kenter JAM 1990 Sedimentol v37, 777-794

MacNeil FS 1954 Amer J Sci v252, 402-427

Paola C et al. 2009 Earth-Sci Rev v.97, 1-43

Rankey EC et al. 2011 J Sed Res v81, 885-900

Reineck HE & Singh IB 1980 Depositional Sedimentary Environments (Springer)

Rietkerk M & Van de Koppel J 2008 Trends Ecol Evol v23/3, 169-175

Schlager W & Purkis 2013 Int J Earth Sci v102, 2225-2238

Schlager W & Purkis 2015 Sedimentol v62, 501-515

Turing AM 1952 Phil Trans Royal Soc London B, v237, 37-72

Van de Koppel J et al. 2005 Amer Naturalist v.165/3, E66-E77

Van de Koppel J et al. 2008 Science v.322, 739-742

Van Wagoner JC et al. 2003 AAPG Search & Discovery #4008